infrastructures

MDPI

Article

Aspects of Vibration-Based Methods for the Prestressing Estimate in Concrete Beams with Internal Bonded or Unbonded Tendons

Angelo Aloisio

Department of Civil, Environmental and Architectural Engineering, Università Degli Studi Dell'Aquila, Via Giovanni Gronchi n.18, 67100 L'Aquila, Italy; angelo.aloisio1@univaq.it

Abstract: The estimate of internal prestressing in concrete beams is essential for the assessment of their structural reliability. Many scholars have tackled multiple and diverse methods to estimate the measurable effects of prestressing. Among them, many experimented with dynamics-based techniques; however, these clash with the theoretical independence of the natural frequencies of the forces of internally prestressed beams. This paper examines the feasibility of a hybrid approach based on dynamic identification and the knowledge of the elastic modulus. Specifically, the author considered the effect of the axial deformation on the beam length and the weight per unit of volume. It is questioned whether the uncertainties related to the estimate of the elastic modulus and the first natural frequency yield reasonable estimates of the internal prestressing. The experimental testing of a set of full-scale concrete girders with known design prestressing supports a discussion about its practicability. The author found that the uncertainty in estimating the natural frequencies and elastic modulus significantly undermines a reliable estimate of the prestressing state.

Keywords: prestress concrete structures; prestressing estimate; nondestructive methods

Citation: Aloisio, A. Discussion on a Vibration-Based Method for the Prestressing Estimate in Concrete Beams with Internal Bonded or Unbonded Tendons. *Infrastructures* **2021**, *6*, 83. https://doi.org/10.3390/infrastructures6060083

Academic Editors: Carlo Rainieri, Andy Nguyen, You Dong and Dmitri Tcherniak

Received: 15 May 2021
Accepted: 1 June 2021
Published: 2 June 2021

1. Introduction: The Role of Prestressing in Structural Reliability

The question of a prestressing estimate may lie between two issues: (1) Is the resisting bending moment of a beam affected by the prestressing force?; (2) Why is the prestress value necessary for the assessment of the structural reliability? The prestressing force does not affect the bending resistance of a prestressed concrete beam: the resistance depends on the resistances of concrete and steel, as depicted in Figure 1, which represents a simplified rectangular cross-section with an eccentric prestressing cable. Likely, the knowledge of the prestressing value is not necessary for the ultimate limit state design inequality:

$$M_{rd} \geq M_{ed} \tag{1}$$

where M_{rd} is the resisting bending moment, and M_{ed} is the bending moment induced by the external loads. However, the prestress force enhances the performance of the beam in operational conditions by reducing its deformability [1] and preventing the cross-section cracking [2–4]. A loss in the prestress force makes the concrete attain tensile stresses with lower load levels. Since the tensile stresses are not admitted or allowed in a limited range, a loss in the prestress force compromises the operational performance of the beam but not its ultimate resistance. The knowledge of the prestressing state is then determined when assessing the maximum admitted loads of a bridge and the performance in operational conditions [5,6].

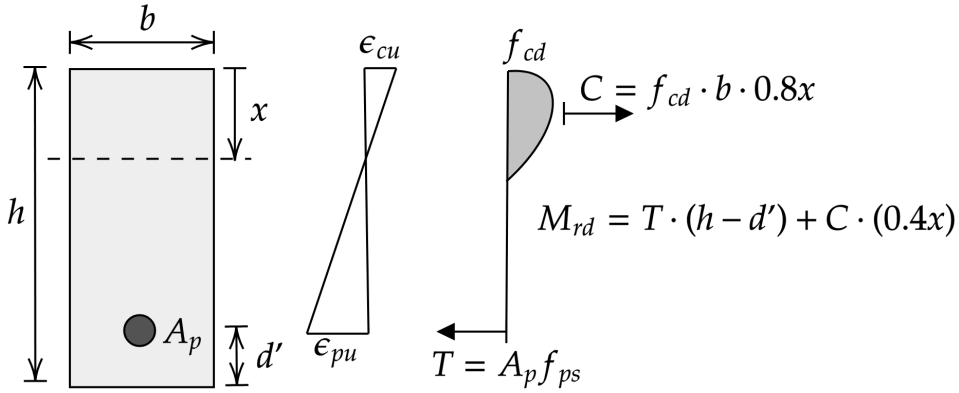

Figure 1. Evaluation of the resisting bending moment of a prestressed beam, where ϵ_{cu} and ϵ_{pu} are the ultimate deformations of concrete and the prestressing cable, f_{cd} is the design concrete stress and f_{ps} is the design tensile stress of the prestressing cable, M_{rd} is the resisting design moment.

2. Efforts in Prestress Estimate

The estimate of prestressing in existing concrete beams is becoming crucial since there is no reliable and widely acknowledged nondestructive method for its estimation [7,8]. Firstly, the author discusses dynamics-based methods; then, they append a brief paragraph about different nondestructive techniques.

2.1. Dynamic-Based Methods

In the last few decades, prestressing techniques have been used to build very important structures, infrastructures, and bridges. Since the serviceability and the safety of prestressed concrete members rely on the effective state of prestressing, the development of tools and dynamic procedures capable of estimating the effective prestress loss have been widely carried on [9–11]. Since the 1970s, many researchers focused on structural dynamics as a possible way to estimate prestressing [12–18]. Vibration-based approaches have been proven successful for damage detection purposes in multiple theoretical analysis and case study analyses [19–22]. However, so far, none have made successful attempts in identifying the internal prestressing forces using vibration-based approaches. The absence of a dynamic-based nondestructive method mainly originates from physical evidence: internal prestressing does not affect the natural frequencies of the beam, and external prestressing has low, barely measurable effects over the natural frequencies. Most of the existing prestressed bridge stocks have internal prestressing.

Recently, Hamed et al. [23] soundly proved the independence of the natural frequencies of internally prestressed beams via a rigorous mathematical approach and condemned the erroneous or unproven formulations by [24–26]. Despite the rigour exhibited in the research paper by [23], the physical reason is unmistakable: internal prestressing is a self-balanced force; see also [27,28]. The total axial force obtained by summing up the tension of steel and the compression of concrete is null. Likely, the beam does not reveal its internal self-balanced stress state, which does not generate effects on the global dynamics. The internal prestressing is concealed and, so far, no one has found a reliable method.

Physics supports any possible way, and experiments have mostly confirmed the absence of measurable effects.

Still, many scholars have found experimental correlations with internal prestressing. Despite the compression softening effect, the authors of [29] discovered a positive nonlinear correlation with increasing internal prestressing. References [30,31] showed significant correlations between the natural frequency and prestressing. Reference [32] found that the natural frequency increases as the prestressing increases.

Lastly, in 2018, Reference [33] solved an inverse problem and identified the stress–strain relationship of concrete, which yielded the experimental findings by [24,29–31].

They concluded that the experimented beams showed a positive correlation between the natural frequency and the prestressing force due to the concrete constitutive behaviour (micro-cracking, nonlinear stress–strain behaviour, etc.). This trend is evident for low values of prestressing level, while higher prestressing lowers the rate of change or produce negative correlations. The author acknowledges the efforts and value of Breccolotti's work. Additionally, many scholars [34–36] strived to persist in experimenting with finite element (FE) methods. They found possible alternatives and obtained some satisfying results, such as [34], who affirmed that a sensitive parameter is a relative ratio of prestressing to the total weight of the structure rather than the prestressing itself.

However, the physics of FE models cannot differ from that of experiments. The faith in progressing technology and computer sciences cannot feed the belief in identifying FE models with real structures. FE models cannot contradict the physical evidence, nor can sophisticated algorithms extract what is proved to have no measurable effect.
Nowadays, it is common practice to tackle physical problems by experimenting using numerical simulation [37]. However, the issue of the prestressing estimate is so delicate that it needs a more traditional approach: firstly, the search for a measurable quantity affected by internal prestressing.

2.2. Other Methods

The most widespread but costly method for testing the operational performance of a beam is the so-called static load test. Static load tests consist of the step-by-step loading of the beam associated with the measurement of the mid-span deflection. The experimenter expects the measurement points to align with a constant slope. The change of slope in the loading curve is generally associated with a reduction of the cross-section inertia due to concrete cracking; hence, the prestressing state can be indirectly obtained by interpolating the load that caused the initial cracking of the cross-section. In addition to vibration-based methods, there are parallel approaches based on acoustoelasticity, static tests, electrical impedance or elastomagnetic effects. In 2019, the authors of [38] reviewed the attempts of identifying and monitoring prestressing forces.

According to the theory of acoustoelasticity, the modulus of elasticity of a material is stress-dependent and increases with the applied compressive stress. References [39,40] successfully identified the prestressing state by exploiting the acoustoelastic effect.

Reference [41] developed a method that can detect the prestress force in a concrete member with a straight unbonded tendon based on second-order static deflections.

The electrical impedance of the piezoelectric actuator is related to the mechanical impedance of the host structure. References [42–44] used the measured electrical impedance to estimate the stress state.

The elastomagnetic methods found the dependence of the magnetic properties of ferromagnetic materials on the mechanical stress, and References [45–47] made successful endeavours.

2.3. Purpose of the Paper: A Diverse Vibration-Based Approach

The current research aims at exploring the effect of axial deformation over the natural frequency of prestressed beams. To the authors' knowledge, no scholar has published results about this effect. This paper shows that the axial deformation might yield measurable outcomes in some situations. The author develops a mathematical formulation of an internal prestressed beam by accounting for the effect of axial deformation over the total length and the mass per unit of volume. Then, they present a hybrid method based on the estimation of the elastic modulus from the static load test and the natural frequency. It is tested how the uncertainty of the elastic modulus and the natural frequency propagates to that of prestressing. Then, in the validation section, the elastic moduli and the natural frequencies estimated from existing concrete box girders yield the approximate estimate of prestressing. The prestressing estimations, compared to the design ones, support the discussion about the method's reliability.

The paper has the following structure: the second section presents the method, and the remaining sections deal with the discussion part regarding a set of full-scale structures.

3. Problem Formulation

The prestressing of concrete, caused by either bonded or unbonded tendons, causes the axial deformation of concrete, $\epsilon_{G,c}$. The axial deformation determines a length reduction and the cross-section expansion due to the Poisson effect, as depicted in Figure 2. In this paper, positive deformations are associated with tensile forces and vice versa. Equation (2) relates the axial deformation of concrete, due to the prestressing force N_c, with the elastic modulus of concrete E_c and the concrete cross-section area A_c.

$$\epsilon_{G,c} = \epsilon_G = \frac{N_c}{E_c \cdot A_c} \tag{2}$$

where ϵ_G is the axial deformation of the beam. The deformation of the beam is not associated with mass variations; hence, the axial deformation affects the weight per unit of volume of the beam. The mass density due to deformation, named ρ_c', may descend from the mass density before the deformation, named ρ_c, by equaling the total mass value before and after the effect of prestressing. Equation (3) equals the total mass of concrete before the deformation with that after the deformation:

$$\rho_c \cdot A_c \cdot l = \rho_c' \cdot \left[(1 - \nu\epsilon_G)^2 \cdot A_c\right] \cdot [(1 + \epsilon_G) \cdot l] \tag{3}$$

where ν is the Poisson ratio. The modification of the mass density of concrete is:

$$\rho_c' = \rho_c \cdot \frac{1}{(1 - \nu\epsilon_G)^2 \cdot (1 + \epsilon_G)} \tag{4}$$

Equation (5) bestows the total mass density, by summing the contributions of concrete and steel.

$$\rho = \rho_c \frac{A_c}{A} + \frac{M_s}{A \cdot l} \quad \rho' = \rho_c' \frac{A_c}{A} + \frac{M_s}{A \cdot [(1 + \epsilon_G) \cdot l]} \tag{5}$$

The total mass of steel is constant and equal to M_s, while A is the cross-section area including the contributions of concrete and steel, and l is the total length of the beam.

This section is based on an elementary mechanical model, a simply supported beam: algebraic equations describe its natural bending frequencies. The axial deformation directly affects the total length of the beam and the total mass density.

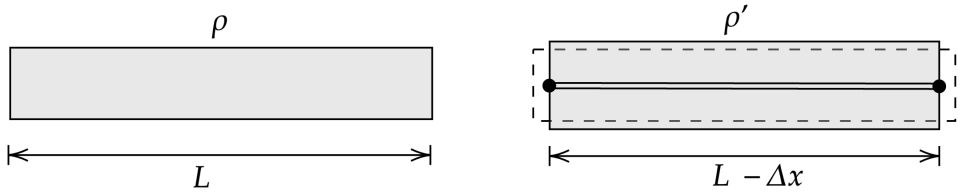

Figure 2. Effect of axial compression in volume contraction.

Equation (6) presents both the natural frequencies of a non-prestressed f_{np} and pre-stressed f_p simply-supported beam:

$$f_{np} = \frac{n^2\pi}{2l^2}\left(\frac{EI}{\rho A}\right)^{0.5} \quad f_p = \frac{n^2\pi}{2(l + \epsilon_G l)^2}\left(\frac{EI}{\rho' A}\right)^{0.5} \tag{6}$$

where I is the cross-section inertia and n is the mode number.

A k factor, explained in Equation (7), shows the relative variation of the natural frequency in a non-prestressed beam due to prestressing.

$$k = \frac{f_p - f_{np}}{f_{np}} \approx \left(1 + \frac{\sigma_c}{E_c}\right)^{-3/2} \left(1 - \nu \frac{\sigma_c}{E_c}\right) - 1 \text{ if } \rho' \approx \rho'_c, \ \rho \approx \rho_c \tag{7}$$

where $\sigma_c = N_c / A$. The approximation of the mass density ($\rho' \approx \rho'_c$, $\rho \approx \rho_c$) aims at simplifying the expression to yield a straightforward interpretation. There are two contributions that act oppositely and do not convey the immediate estimation of the sign of the expression. In the case of negative axial deformations, the reduction of the total length may increase the natural frequencies by reducing the free vibration length. Reversely, the compression yields an increment of the mass density, which should cause the reduction of the natural frequency. Interestingly, the k factor is independent of the cross-section characteristics and the total length of the beam: it depends on three variables, the concrete stress σ_c due to prestressing, the elastic modulus of concrete E_c and the Poisson ratio, ν, see Equation (8).

$$k = k(E_c, \sigma_c, \nu) \tag{8}$$

In practical situations, the Poisson ratio can be considered as known, and σ_c and E_c are the significant variables. Figure 3 plots Equation (7) in a range of variations possibly consistent with practical situations; the concrete stress spans between -100 and 100 MPa, and the elastic modulus ranges between 15,000 and 40,000 MPa. The plots reveal an inverse phenomenon to that observed about external prestressing, i.e., the compression softening effect. In this situation, compression determines a rising of the natural frequencies, while tension is lowering. Likely, prestressing yields a sort of "compression hardening". The neologism "compression hardening" indicates the increment of the natural frequencies due to internal prestressing, as if concrete exhibited a sort of hardening effect.

Figure 3 may convey the following evidence:

- Compression stresses determine the increase of the natural frequencies, likely affecting the hardening of concrete. Tension stresses determine the lowering of the natural frequencies, likely affecting the softening concrete. The author will refer to the two phenomena as "compression hardening" and "tension softening effect". This effect is opposite to that caused by external prestressing, which induces the so-called "compression softening" effect;
- The relative variation of the natural frequencies due to prestressing range between -1 and 1% in an interval between -100 and 100 MPa. In ordinary prestressed structures, where concrete may have a -50 MPa compression, the frequency increment is about 0.5%;
- Equation (7) depends on the sole axial deformation, expressed by the ratio σ_c / E_c. The contour plot in Figure 3 is then invariant to the σ_c / E_c ratio;
- The functional dependence between the relative frequency variation and σ_c is practically linear in the range of interest;
- Natural frequencies can be measured with extreme accuracy, up to the fourth decimal place. The "compression hardening" effect may yield a measurable effect over the natural frequencies.

It must be remarked that, theoretically, when the axial force acting in one direction reaches a critical value, the vibration stops. Conversely, when the axial force acts perpendicularly to the cross-section and the cross-section experiences rotation with force, the frequency of vibrations increases with force. Additionally, the axial force can change direction during vibration due to the rotation of the cross-section.

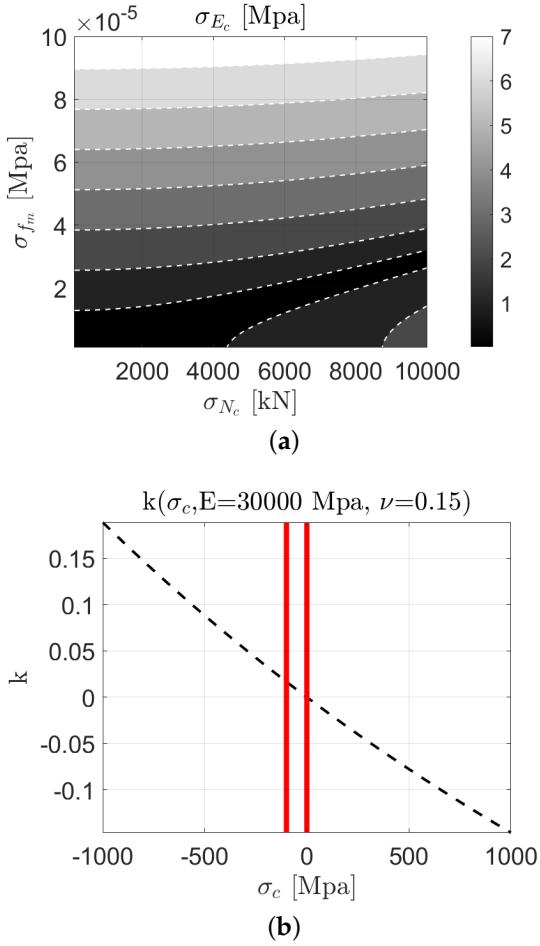

Figure 3. Percentage variation of the natural frequency expressed by the approximate k ratio in Equation (7). (**a**) The variation of both E and σ_c; (**b**) the dependence of the k factor on the natural sole compression stress given the elastic modulus. The solid vertical lines in (**b**) indicate the range of interest in existing concrete structures, averaging between −100 and 0 MPa.

3.1. Comparison between the "Compression Hardening" and "Compression Softening"

The effect of the axial deformation on the beam length and the mass density also affect beams with external prestressing. Equation (9) expresses the natural frequency of a simply-supported beam, compressed by two external forces N_c. Equation (9) considers both the compression softening effect due to external prestressing and that counted in Equation (6).

$$f_{ep} = \frac{n^2\pi}{2(l+\epsilon_G l)^2}\left(\frac{EI}{\rho' A}\right)^{0.5}\left(1+\frac{N_c l^2}{\pi^2 EI}\right)^{0.5} \tag{9}$$

Equation (10) defines the relative variation of the natural frequency due to prestressing. In contrast with Equation (7), the h ratio depends on the beam inertia and the total axial force.

$$h = \frac{f_{ep}-f_{np}}{f_{np}} \approx \left(1+\frac{\sigma_c}{E_c}\right)^{-3/2}\cdot\left(1-\nu\frac{\sigma_c}{E_c}\right)\cdot\left(1+\frac{N_c l^2}{\pi^2 EI}\right)^{0.5}-1 \tag{10}$$

The author compared the compression softening to the compression hardening in two sample cases to merely understand the magnitude of the effects. Figure 4 proves that the compression softening effect, ranging between 0–4%, is on average higher than the hardening one, between 0–1%. The absolute ratio between h and k is nearly constant

and spans between 73 and 74. In conclusion, higher prestressing forces magnifies the compression softening effect.

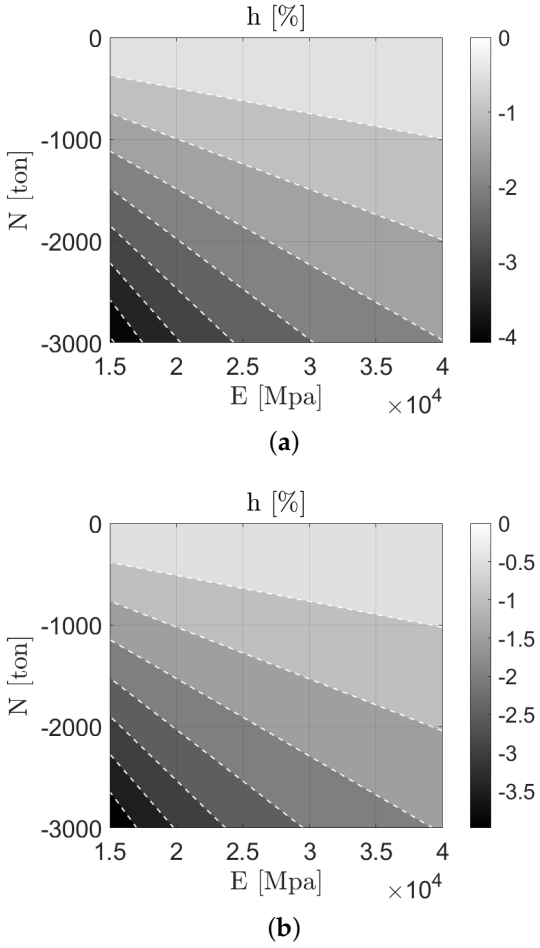

Figure 4. Percentage variation of the natural frequency in externally prestressed beams expressed by the *h* ratio in Equation (10), given two sample cases (**a**) with A = 6 m^2, I = 4 m^4, ν = 0.2, ρ = 2500 kg/m^3 and (**b**) with A = 2 m^2, I = 4 m^4, ν=0.2, ρ = 2500 kg/m^3.

3.2. General Formulation

This part proves that the effect of prestressing can be easily considered under boundary conditions different from those treated in the previous section. Equations (11) and (12) describe the transversal and axial dynamics of a planar beam, according to the Euler–Bernoulli theory.

$$EI\frac{\partial^4 v}{\partial x^4} + \rho\frac{\partial^2 v}{\partial t^2} = 0 \tag{11}$$

$$EA\frac{\partial^2 u}{\partial x^2} + \rho\frac{\partial^2 u}{\partial t^2} = 0 \tag{12}$$

v is the transversal displacement, u is the axial displacement, x is the abscissa spanning the length of the beam, and t is the time. In the classical formulation, both the bending stiffness and the mass density are constant. Equations (11) and (12) describe the equilibrium of a planar beam by considering the effect of axial deformation on the value of the mass density. This effect couples the two equations, uncoupled in the Euler–Bernoulli formulation.

$$EI\frac{\partial^4 v}{\partial x^4} + \rho \cdot \left[(1-\nu\frac{\partial u}{\partial x})^2 \cdot (1+\frac{\partial u}{\partial x})\right]^{-1}\frac{\partial^2 v}{\partial t^2} = 0 \tag{13}$$

$$EA\frac{\partial^2 u}{\partial x^2} + \rho \cdot \left[(1 - \nu\frac{\partial u}{\partial x})^2 \cdot (1 + \frac{\partial u}{\partial x})\right]^{-1} \frac{\partial^2 u}{\partial t^2} = 0 \tag{14}$$

Equations (11) and (12) are nonlinear partial differential equations. However, the coupling term is constant in the case of uniform prestressing; Equation (13) returns uncoupled, but has a different mass density. Equations (13) and (14) confirm that the effect of prestressing can be easily considered in different boundary conditions, as the one tested in the previous paragraph, by solving the homogeneous equation.

4. Method

The possible negligible but explicit dependence of the natural frequencies on the prestressing force may endorse an attempt for its estimation. The identification problem is a classical optimization: minimizing an objective function. The objective function is the difference between the natural frequency of the prestressed beam according to the formulation in Equation (13), while f_m is the natural frequency measured in situ.

$$g(N_c) = \sum_i^n f_{p,i} - f_{m,i} = 0 \tag{15}$$

where i indicates the mode number, while n is the total number of modes. The minimum of Equation (15) yields an estimate of the prestressing force. Equation (16) explicates the dependence of the estimated N_c on three sets of variables, related to the cross-section geometry, the material constitutive behaviour and the experimental natural frequencies.

$$N_c = f(\{A, I\}_1, \{E_c, \nu, \rho\}_2, \{f_m\}_3) \tag{16}$$

The three sets of variables are associated with distinct levels of uncertainty. While the geometry of the cross-section can be known precisely from an accurate survey, the material and the experimental outcomes may be affected by a higher uncertainty. According to the author, among them, three variables may suffer from the highest level of uncertainty: the elastic modulus of concrete E_c, and the experimental frequency f_m. The uncertainties associated with the three variables propagate to the prestress estimate. The assessment of the role of each variable is essential to understand the feasibility of the approach.

Quantification of the Uncertainty

From a statistical point of view, there are three types of errors on the estimated prestressing:

- Bias of the mechanical model: the model is not entirely representative of the tested structure;
- Bias of the input variables: the estimates of the material property or natural frequencies may be biased;
- Variance of the input variables: the estimates of the material property or the natural frequencies may have variance errors.

At this stage, the author will ignore the bias error, which can be partially removed in many occurrences. Otherwise, the variance errors can only be estimated, but not removed. The author will assess the variance error of the prestressing estimates by using a linear sensitivity analysis. The first-order Taylor expansion of Equation (16) is:

$$N_c \approx f^0 + \sum_i^3 \frac{\partial f}{\partial x_i} x_i \tag{17}$$

where $\frac{\partial f}{\partial x_i}$ denotes the partial derivative of f with respect to the i-th variable, evaluated at the mean value of x. In matrix notation:

$$N_c \approx f^0 + Jx \tag{18}$$

where J is the Jacobian matrix, while x collects all the x_i variables. The propagation of the variance can be written as:

$$\Sigma^{N_c} = J\Sigma^x J^T \tag{19}$$

where Σ^{N_c} and Σ^x are the covariance matrices.

Rather than assessing the propagation of variance, the author thinks that the inverse problem should deserve more attention at this step. Which variances of input variables yield an estimate of prestressing within acceptable bounds?

In the next section, the estimates of prestressing on existing concrete bridges are associated with the estimation of the admitted confidence values of the elastic modulus to yield a possibly reliable estimate.

5. Testing of the Procedure on a Real Case Problem

In 2019, the author carried out the dynamic identification of a set of seven prestressed concrete girders. The girders have a hollow cross-section and are 40 m long. Ten force-balance accelerometers (FBA) measured the deck response to ambient excitation. The recordings, sampled at 200 Hz, lasted approximately 40 min. The Stochastic-Subspace Identification (SSI) method returned an estimate of the modal parameters [48–50]. The reader might find sufficient details about the girders, the experimental setup and the results of operational modal analysis in the following research papers [50–52]. The author will avoid replicating the same information reported in these papers by focusing on the prestressing estimate.

This manuscript lacks a proper validation section on multiple laboratory girders with known prestressing. However, the discussion based on the seven girders may have some merit; the girders are operational and representative of the uncertainties of real applications. Such applications comprise uncertainties of which laboratory tests cannot easily replicate.

The seven girders are nominally identical with the same design prestressing. Additionally, the static load test confirmed that the actual prestressing losses are not higher than 30% of the design prestressing N_d. This information will be the basis of the discussion. The following questions are answered: does the prestressing estimate fall within the expected range of variation $N_d \pm 30\%$? Which variances of the variables can generate the assumed confidence bounds, $N_d \pm 30\%$? The variances of the measured natural frequencies are known. They originate from the procedure described by [53]. The sole variable with unknown variance is the elastic modulus of concrete.

The purpose of this section is then the estimation of the prestressing forces and the boundary values of the elastic modulus associated with a 30% variation of prestressing by assuming the variance of the natural frequencies as known.

Results

The author solved the optimization problem described in Equation (15) by using the input parameters in Table 1 and the experimental values in Table 2; the first natural frequency and the elastic modulus from the static load test. The use of the first natural frequency depends on the good accordance between the first mode shape and that of a simply supported beam, as remarked in [52]. This supports the use of Equation (6) in Equation (15). Table 2 details the resulting prestressing values obtained from the elastic moduli estimated with static load tests and concrete specimens.

The prestressing values obtained from Equation (15) are far beyond the actual prestress state, and the estimates are entirely unreliable.

As a second step, the author estimated the elastic moduli, which would yield the design prestressing N_d = 29,000 kN, by using the same parameters reported in Tables 2 and 3. Table 2 shows the elastic moduli associated with the design prestressing and those corresponding to a 30% variation of prestressing. An estimate of prestressing within 30% confidence bounds would require the elastic modulus to have a maximum deviation of 3 MPa from the mean.

Table 1. Characteristics of the girders.

ρ [kg/m^3]	2500
A [m^2]	6
I [m^4]	4
l [m]	40

Table 2. Outcomes of the experimental tests on the prestressed concrete girders. Static T. stands for static test, Concr. Samp. stands for concrete samples.

Viaduct	Span	Elastic Modulus (MPa)		Estimated Prestressing (kN)		f_m	σ_{f_m}
		Static T.	Concr. Samp.	Static T.	Concr. Samp.		
Biselli	12	24,900	/	18,811,320	/	2.655	2.00×10^{-4}
Cerchiara	4	15,000	19,361	17,076,890	11,105,390	2.967	2.15×10^{-3}
Cerchiara	7	23,700	23,299	19,959,130	20,501,280	2.678	1.50×10^{-4}
Cretara	9	26,000	26,416	44,637,030	44,540,770	3.564	1.50×10^{-4}
Le Grotte	5	36,000	/	−3,930,700	/	2.661	2.00×10^{-4}
San Nicola	10	26,700	29,978	17,808,040	11,932,910	2.683	3.50×10^{-3}
Temperino	6	35,900	/	−16,558,670	/	2.515	5.00×10^{-5}

Table 3. Elastic moduli associated with the design prestressing N_d = 29,000 kN.

Viaduct	Elastic Moduli Yielding N_c within ± 30% (MPa)			
	$E_c(0.7 \cdot N_d)$	$E_c(1.3 \cdot N_d)$	$E_c(N_d)$	ΔE_{max}
Biselli	27,367	27,373	27,370	6
Cerchiara	19,638	19,644	19,641	6
Cerchiara	27,875	27,881	27,878	6
Cretara	45,347	45,353	45,350	6
Le Grotte	27,554	27,560	27,557	6
San Nicola	28,224	28,230	28,227	6
Temperino	23,994	24,000	23,997	6

The design prestressing value is associated with elastic moduli not significantly different from that obtained from static load tests. However, a moderate variation in the elastic modulus generates a considerable variation of the estimated prestressing, as shown in Figure 5a. Figure 5a depicts the estimate of prestressing as a function of the elastic modulus in the case of the Biselli bridge span. The visualization of the dot representative of the elastic modulus corresponding to the design prestressing requires the focusing in Figure 5b.

The results of this analysis remark the considerable sensitivity of the prestress estimate on the elastic modulus. The natural frequencies can be obtained with high accuracy ($\approx 10^{-4}$), but the same accuracy does not belong to the estimates of the elastic modulus in working situations. The values from static load tests do not discern the tenths of the measure, while the values from concrete samples are generally scattered, with a variance far higher than 3 MPa.

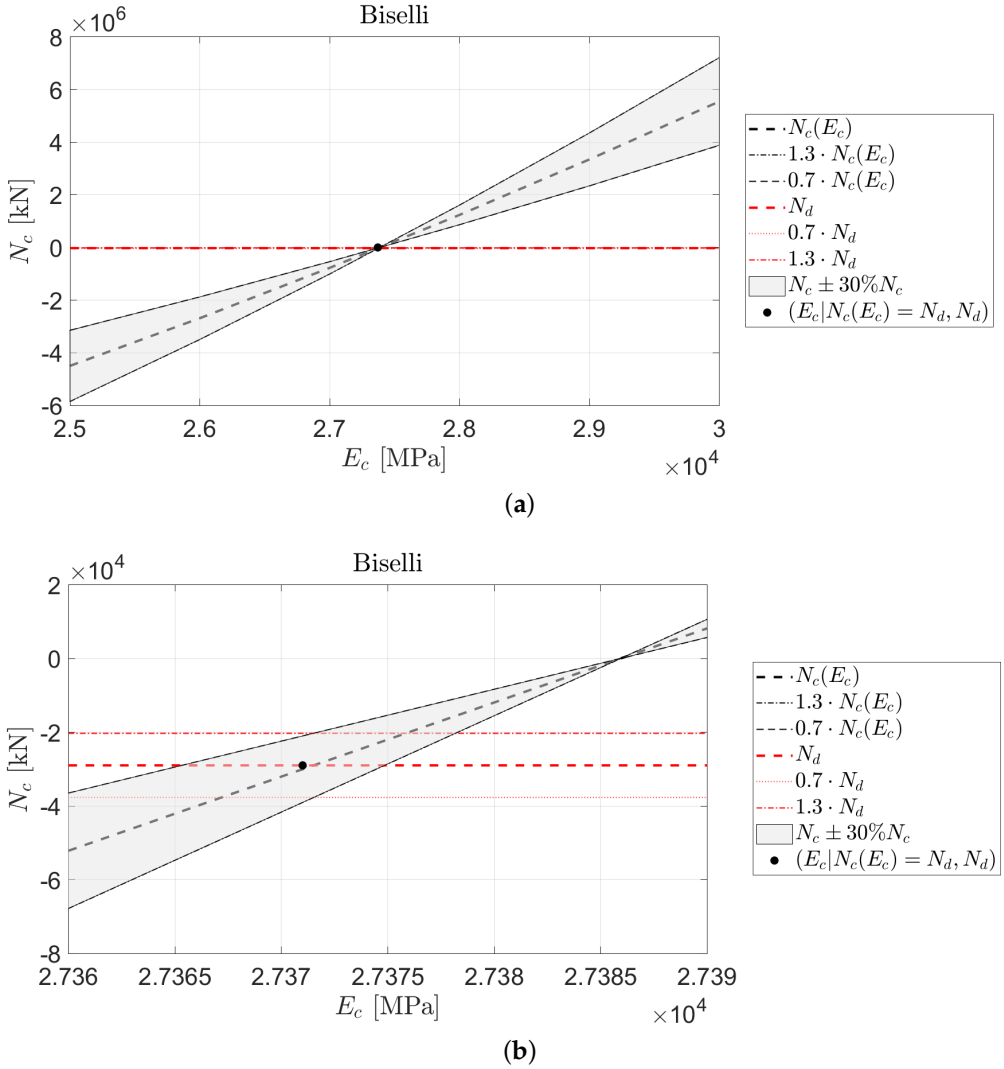

Figure 5. Estimated values of the elastic modulus to yield the design prestressing value within the given ±30% confidence bounds: (**a**) spans between 25,000 and 30,000 MPa, (**b**) focuses on the estimated value.

The variance of the elastic modulus given by the variances of the natural frequency and the prestress force may provide useful information about the required level of resolution in the elastic modulus estimate to yield reliable results. If the elastic modulus and the natural frequency are uncorrelated variables, the variance of the prestress estimate can be approximated by:

$$\sigma^2_{N_c} \approx \left(\frac{\partial f}{\partial f_m}\right)^2 \sigma^2_{fm} + \left(\frac{\partial f}{\partial E_c}\right)^2 \sigma^2_{E_c} \tag{20}$$

Figure 6 shows the contour plot of the variance of the elastic modulus σ_{E_c}, given σ^2_{fm} and $\sigma^2_{N_c}$, estimated from Equation (20). Interestingly, σ_{E_c} does not strongly depend on the confidence bounds of prestressing given a certain variance of the natural frequency. Furthermore, σ_{E_c} grows almost linearly as the variance of the natural frequency increases.

Still, a reliable estimate of N_c would require a very high resolution of E_c, not exceeding 7 MPa.

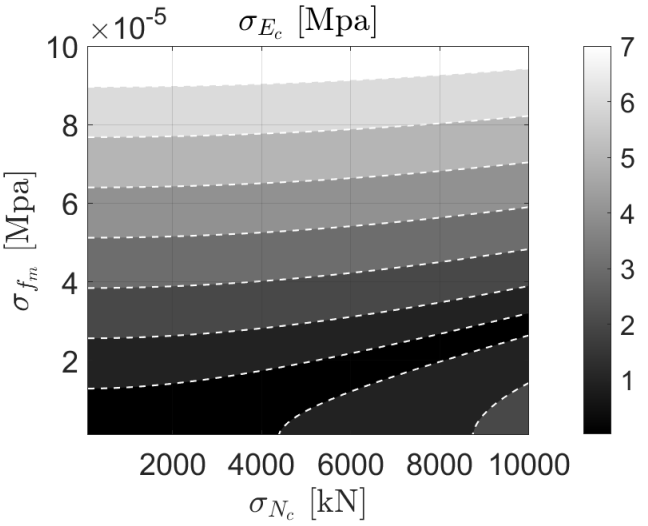

Figure 6. Variance of the elastic modulus associated with the variances of prestressing and the first natural frequency, ranging between 0–10,000 kN and 10^{-5}–10^{-4} MPa, respectively.

6. Discussion

The effect of the axial deformation in the estimate of the prestressing forces does not return reliable estimates if the geometric and mechanical properties of the beam are not known with sharp precision. While the experimental variances of the natural frequencies can be considerably low, that of the elastic modulus does not have the same accuracy due to several causes. The estimates of the elastic modulus from the static load test do not have sufficient resolution. Additionally, concrete is not an entirely homogeneous material; the mechanical properties of concrete change from point to point, and the elastic modulus, within the same beam, may have a scatter higher than the required interval for a reliable estimate of prestressing. In conclusion, the method reveals to be unreliable.

Still, the author experimented the feasibility of the technique on the first natural frequency. The frequency shift due to the axial deformation increases when attaining higher modes. Precisely, the acoustic emission of a beam may be read profitably in light of this effect. The author will aim at experimenting with the method on higher modes by exploiting alternative methods to estimate the elastic modulus based on more accurate methods, like the ones based on the longitudinal wave propagation.

7. Conclusions

The author tested the effect of the axial deformation due to internal prestressing on the estimate of the prestressing force. The axial deformation affects the beam length and mass density. Hence, the natural frequencies can be written as a function of the prestressing state. The prestress forces may descend by solving an elementary optimization problem. The method requires the knowledge of the geometrical and mechanical properties of the beam in terms of cross-section area and inertia, elastic modulus, Poisson ratio and experimental natural frequencies. Additionally, the method further requires the precise knowledge of the boundary conditions not to have a biased mechanical model, representative of the beam dynamics. The procedure is tested on a set of seven simply-supported prestressed concrete girders, using the first experimental natural frequency. The elastic modulus of the seven girders descended from static load tests, whereas the natural frequencies were from the operational modal analysis. Regrettably, the outcomes of the method are not reliable; the estimated values enormously exceed the expected prestressing. The main reason for the method's deficiency is found in the significant sensitivity of the estimates on the elastic modulus. A reliable estimate would require extremely sharp precision of the elastic modulus, which is difficult to attain given the intrinsic scatter within the same beam and the measurement limits. Still, the effect of frequency variation is considerable at higher frequencies. The author will attempt to test this method at higher modes by using a different

and more accurate procedure to measure the elastic modulus. Additionally, he aims at testing the effect of the prestressing state on the elastic modulus of concrete via extensive experimental tests and detailed modelling of the concrete nonlinear constitutive behaviour.

Funding: This research received no external funding.

Data Availability Statement: Some or all data, models, or code that support the findings of this study are available from the corresponding author upon reasonable request.

Conflicts of Interest: The author declares no conflict of interest.

References

1. Bažant, Z.P.; Yu, Q.; Li, G.H. Excessive long-time deflections of prestressed box girders. I: Record-span bridge in Palau and other paradigms. *J. Struct. Eng.* **2012**, *138*, 676–686. [CrossRef]
2. Guo, W.; Liang, P.; Liu, H.; Chen, Y.F.; Zhao, X. An Evaluation Method for Effective Prestress of Simply Supported Prestressed Concrete Beams with Breathing Cracks. *Adv. Civil. Eng.* **2021**, *2021*, 8876093. [CrossRef]
3. Almohammedi, A.; Murray, C.D.; Dang, C.N.; Hale, W.M. Investigation of measured prestress losses compared with design prestress losses in AASHTO Types II, III, IV, and VI bridge girders. *PCI J.* **2021**, *66*, 32–48. [CrossRef]
4. Zhou, W.; Li, H.; Zhang, W. Experimental behavior of the shear strength of full-scale precast prestressed double tees. *J. Build. Eng.* **2021**, *42*, 102455. [CrossRef]
5. Caro, L.; Martí-Vargas, J.R.; Serna, P. Prestress losses evaluation in prestressed concrete prismatic specimens. *Eng. Struct.* **2013**, *48*, 704–715. [CrossRef]
6. Chung, W.; Kim, S.; Kim, N.S.; Lee, H.u. Deflection estimation of a full scale prestressed concrete girder using long-gauge fiber optic sensors. *Constr. Build. Mater.* **2008**, *22*, 394–401. [CrossRef]
7. Botte, W.; Vereecken, E.; Taerwe, L.; Caspeele, R. Assessment of posttensioned concrete beams from the 1940s: Large-scale load testing, numerical analysis and Bayesian assessment of prestressing losses. *Struct. Concr.* **2021**. [CrossRef]
8. Huynh, T.C.; Kim, J.T. FOS-based prestress force monitoring and temperature effect estimation in unbonded tendons of PSC girders. *J. Aerosp. Eng.* **2017**, *30*, B4016005. [CrossRef]
9. Bonopera, M.; Chang, K.; Ou, Y. Overview on the prestress loss evaluation in concrete beams. In *Bridge Maintenance, Safety, Management, Life-Cycle Sustainability and Innovations*; CRC Press: Boca Raton, FL, USA, 2021; pp. 117–122.
10. Modano, M.; Fabbrocino, F.; Gesualdo, A.; Matrone, G.; Farina, I.; Fraternali, F. On the forced vibration test by vibrodyne. In Proceedings of the COMPDYN 2015 Conference Proceedings, Crete Island, Greece, 25–27 May 2015; pp. 25–27.
11. Páez, P.M.; Sensale-Cozzano, B. Time-dependent analysis of simply supported and continuous unbonded prestressed concrete beams. *Eng. Struct.* **2021**, *240*, 112376. [CrossRef]
12. Adams, R.; Cawley, P.; Pye, C.; Stone, B. A vibration technique for non-destructively assessing the integrity of structures. *J. Mech. Eng. Sci.* **1978**, *20*, 93–100. [CrossRef]
13. Stubbs, N.; Osegueda, R. Global non-destructive damage evaluation in solids. *Int. J. Anal. Exp. Modal Anal.* **1990**, *5*, 67–79.
14. Doebling, S.W.; Farrar, C.R.; Prime, M.B. A summary review of vibration-based damage identification methods. *Shock Vib. Dig.* **1998**, *30*, 91–105. [CrossRef]
15. Kim, J.T.; Yun, C.B.; Ryu, Y.S.; Cho, H.M. Identification of prestress-loss in PSC beams using modal information. *Struct. Eng. Mech.* **2004**, *17*, 467–482. [CrossRef]
16. Miyamoto, A.; Tei, K.; Nakamura, H.; Bull, J.W. Behavior of prestressed beam strengthened with external tendons. *J. Struct. Eng.* **2000**, *126*, 1033–1044. [CrossRef]
17. Law, S.; Lu, Z. Time domain responses of a prestressed beam and prestress identification. *J. Sound Vib.* **2005**, *288*, 1011–1025. [CrossRef]
18. Ghaemdoust, M.R.; Wang, F.; Li, S.; Yang, J. Numerical Investigation on the Transverse Vibration of Prestressed Large-Span Beams with Unbonded Internal Straight Tendon. *Materials* **2021**, *14*, 2273. [CrossRef]
19. Aloisio, A.; Di Battista, L.; Alaggio, R.; Fragiacomo, M. Sensitivity analysis of subspace-based damage indicators under changes in ambient excitation covariance, severity and location of damage. *Eng. Struct.* **2020**, *208*, 110235. [CrossRef]
20. Alaggio, R.; Aloisio, A.; Antonacci, E.; Cirella, R. Two-years static and dynamic monitoring of the santa maria di collemaggio basilica. *Constr. Build. Mater.* **2021**, *268*, 121069. [CrossRef]
21. Aloisio, A.; Di Pasquale, A.; Alaggio, R.; Fragiacomo, M. Assessment of seismic retrofitting interventions of a masonry palace using operational modal analysis. *Int. J. Archit. Herit.* **2020**. [CrossRef]
22. Aloisio, A.; Alaggio, R.; Fragiacomo, M. Bending Stiffness Identification of Simply Supported Girders using an Instrumented Vehicle: Full Scale Tests, Sensitivity Analysis, and Discussion. *J. Bridge Eng.* **2021**, *26*, 04020115. [CrossRef]
23. Hamed, E.; Frostig, Y. Natural frequencies of bonded and unbonded prestressed beams—prestress force effects. *J. Sound Vib.* **2006**, *295*, 28–39. [CrossRef]
24. Saiidi, M.; Douglas, B.; Feng, S. Prestress force effect on vibration frequency of concrete bridges. *J. Struct. Eng.* **1994**, *120*, 2233–2241. [CrossRef]
25. Raju, K.K.; Rao, G.V. Free vibration behavior of prestressed beams. *J. Struct. Eng.* **1986**, *112*, 433–437. [CrossRef]

26. Kerr, A.D. On the dynamic response of a prestressed beam. *J. Sound Vib.* **1976**, *49*, 569–573. [CrossRef]
27. Deák, G. Discussion of "Prestress Force Effect on Vibration Frequency of Concrete Bridges" by M. Saiidi, B. Douglas, and S. Feng. *J. Struct. Eng.* **1996**, *122*, 458–459. [CrossRef]
28. Materazzi, A.; Breccolotti, M.; Ubertini, F.; Venanzi, I. Experimental modal analysis for assessing prestress force in PC bridges: A sensitivity study. In Proceedings of the 3rd International Operational Modal Analysis Conference, Portonovo, Italy, 4–6 May 2009; Curran Associates, Inc.: Portonovo, Italy, 2009.
29. Kim, B.H.; Jang, J.B.; Lee, H.P.; Lee, D.H. Effect of prestress force on longitudinal vibration of bonded tendons embedded in a nuclear containment. *Nucl. Eng. Des.* **2010**, *240*, 1281–1289. [CrossRef]
30. Jang, J.B.; Lee, H.P.; Hwang, K.M.; Song, Y.C. A sensitivity analysis of the key parameters for the prediction of the prestress force on bonded tendons. *Nucl. Eng. Technol.* **2010**, *42*, 319–328. [CrossRef]
31. Wang, T.H.; Huang, R.; Wang, T.W. The variation of flexural rigidity for post-tensioned prestressed concrete beams. *J. Mar. Sci. Technol.* **2013**, *21*, 300–308.
32. Noh, M.H.; Seong, T.R.; Lee, J.; Park, K.S. Experimental investigation of dynamic behavior of prestressed girders with internal tendons. *Int. J. Steel Struct.* **2015**, *15*, 401–414. [CrossRef]
33. Breccolotti, M. On the evaluation of prestress loss in PRC beams by means of dynamic techniques. *Int. J. Concr. Struct. Mater.* **2018**, *12*, 1. [CrossRef]
34. Shin, S.; Kim, Y.; Lee, H. Effect of prestressing on the natural frequency of PSC bridges. *Comput. Concr.* **2016**, *17*, 241–253. [CrossRef]
35. Li, J.; Zhang, F. Experimental research and numerical simulation of influence of pre-stress values on the natural vibration frequency of concrete simply supported beams. *J. Vibroeng.* **2016**, *18*, 4592–4604. [CrossRef]
36. Kovalovs, A.; Rucevskis, S.; Akishin, P.; Kolupajevs, J. Numerical Investigation on Detection of Prestress Losses in a Prestressed Concrete Slab by Modal Analysis. In Proceedings of the IOP Conference Series: Materials Science and Engineering, Busan, Korea, 25–27 August 2017; Volume 251.
37. Biswal, S.; Reddy, D.; Ramaswamy, A. Reducing uncertainties in estimating long-time prestress losses in concrete structures using a hygro-thermo-chemo-mechanical model for concrete. *Comput. Struct.* **2019**, *211*, 1–13. [CrossRef]
38. Abdel-Jaber, H.; Glisic, B. Monitoring of long-term prestress losses in prestressed concrete structures using fiber optic sensors. *Struct. Health Monit.* **2019**, *18*, 254–269. [CrossRef]
39. Lundqvist, P.; Rydén, N. Acoustoelastic effects on the resonance frequencies of prestressed concrete beams—Short-term measurements. *Ndt Int.* **2012**, *50*, 36–41. [CrossRef]
40. Chen, L.Y.; Liu, Y. Acoustic characteristic analysis of prestressed cylindrical shells in local areas. *Int. J. Acoust. Vib.* **2016**, *21*, 301–307. [CrossRef]
41. Bonopera, M.; Chang, K.C.; Chen, C.C.; Sung, Y.C.; Tullini, N. Feasibility study of prestress force prediction for concrete beams using second-order deflections. *Int. J. Struct. Stab. Dyn.* **2018**, *18*, 1850124. [CrossRef]
42. Pham, Q.Q.; Dang, N.L.; Kim, J.T. Piezoelectric Sensor-Embedded Smart Rock for Damage Monitoring in a Prestressed Anchorage Zone. *Sensors* **2021**, *21*, 353. [CrossRef]
43. Kaur, N.; Goyal, S.; Anand, K.; Sahu, G.K. A cost-effective approach for assessment of pre-stressing force in bridges using piezoelectric transducers. *Measurement* **2021**, *168*, 108324. [CrossRef]
44. Ryu, J.Y.; Huynh, T.C.; Kim, J.T. Tension force estimation in axially loaded members using wearable piezoelectric interface technique. *Sensors* **2019**, *19*, 47. [CrossRef] [PubMed]
45. Fabo, P.; Jarosevic, A.; Chandoga, M. Health monitoring of the steel cables using the elasto-magnetic method. In Proceedings of the ASME International Mechanical Engineering Congress and Exposition, New Orleans, LA, USA, 17–22 November 2012; Volume 36258, pp. 295–299.
46. Ansari, F. *Sensing Issues in Civil Structural Health Monitoring*; Springer: Berlin/Heidelberg, Germany, 2005.
47. Zonta, D.; Esposito, P.; Molignoni, M.; Zandonini, R.; Wang, M.; Zhao, Y.; Yim, J.; Gorriz, B.T. Calibration of elasto-magnetic sensors for bridge-stay cable monitoring. In Proceedings of the Sixth European Workshop on Structural Health Monitoring, Dresden, Germany, 3–6 July 2012; Volume 2012.
48. Peeters, B.; De Roeck, G. Reference-based stochastic subspace identification for output-only modal analysis. *Mech. Syst. Signal Process.* **1999**, *13*, 855–878. [CrossRef]
49. Rainieri, C.; Fabbrocino, G. *Operational Modal Analysis of Civil Engineering Structures*; Springer: New York, NY, USA, 2014; Volume 142, p. 143.
50. Aloisio, A.; Pasca, D.; Tomasi, R.; Fragiacomo, M. Dynamic identification and model updating of an eight-storey CLT building. *Eng. Struct.* **2020**, *213*, 110593. [CrossRef]
51. Aloisio, A.; Alaggio, R.; Fragiacomo, M. Time-domain identification of elastic modulus of simply supported box girders under moving loads: Method and full-scale validation. *Eng. Struct.* **2020**, *215*, 110619. [CrossRef]
52. Aloisio, A.; Pasca, D.P.; Alaggio, R.; Fragiacomo, M. Bayesian estimate of the elastic modulus of concrete box girders from dynamic identification: a statistical framework for the A24 motorway in Italy. *Struct. Infrastruct. Eng.* **2020**, 1–13. [CrossRef]
53. Reynders, E.; Pintelon, R.; De Roeck, G. Uncertainty bounds on modal parameters obtained from stochastic subspace identification. *Mech. Syst. Signal Process.* **2008**, *22*, 948–969. [CrossRef]